Synthesis, Characterization, and Biological Reactivities of Metal Saphen Complexes

Honors Research Thesis

Presented in partial fulfillment of the requirements for graduation *with honors research distinction* in Chemistry in the undergraduate College of Arts and Sciences of the Ohio State University

By

Andrei Jipa

The Ohio State University
May 2014

Project Advisor: Professor James Cowan, Department of Chemistry

Background

Salen, the imine formed by the condensation of salicylaldehyde and ethylenediamine, is a common and well-known ligand in the formation of transition metal complexes. Imine condensation is characterized by the formation of a carbon-nitrogen double bond. Saphen, or Salphen, ligands are formed by a similar condensation reaction between salicylaldehyde and *o*-phenylenediamine, or their derivatives. The primary difference between salen and saphen is the presence of a benzene ring from *o*-phenylenediamine (Fig. 1). Increased scientific interest in saphen complexes has arisen in the past 30 years. While initial studies observed the fluorescence of metal saphen complexes, it was their ability to catalyze oxidation reactions on organic substrates that brought the recent increase in interest. Mn (saphen) derivatives, of which one of the best known is Jacobsen's catalyst, are used in asymmetric epoxidation (Shitama 2006). In addition, Cr(saphen) derivatives have been reported to catalyze the oxidation of benzyl alcohol (Wu 2013) and V(saphen) oxide dervitives similarly catalyze the oxidation of thioethers to sulfoxides (Coletti 2012).

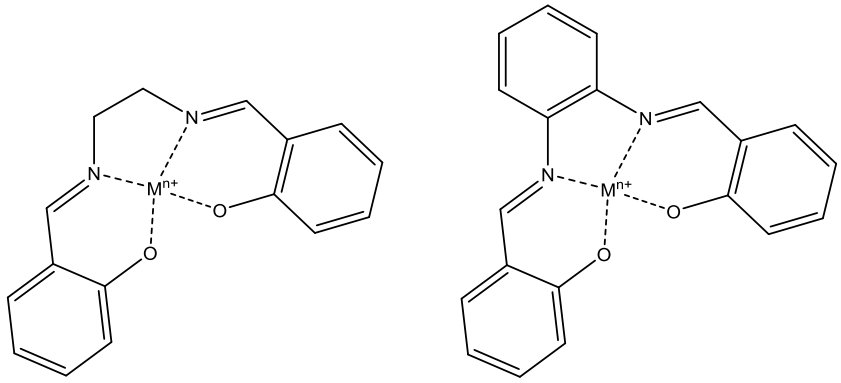

Metal Salen Complex Metal Saphen Complex

M^{n+}=positively charged transition metal

Figure 1. Metal Salen and Saphen Complexes

These catalytic properties combined with the ability of the planar, pi-conjugated ligand to intercalate DNA led to further interest in biological applications of saphen complexes. Fe(saphen) was found to complex plasmid DNA and induce cleavage in the presence of the reducing agent DTT. (Woldemarian 2008). Zn(saphen) complexes will also complex plasmid DNA (Gianicchi 2013). This ability to intercalate and cleave plasmid is interesting because, like a biological enzyme, the ligand "targets" the reactive metal center to DNA.

In addition to work on the complexation of and cleavage of plasmid DNA, the interaction between saphen complexes and G-quadruplexes has also been investigated. The G-quadruplex is a particular type of quadruple-stranded DNA held together by non-canonical Hogsteen base pairing which is found in the telomeres of eukaryotic cells. It is known that Cu(saphen) derivatives stabilize the the G-quadruplex by intercalation. This interaction has been observed through UV-Visible spectroscopy and DNA melting temperature experiments (Li 2013, Bahaffi 2012) as well as x-ray crystallography of the complexed G-quadruplex (Campbell 2011). In these experiments, naphthalene diamines were used as a substitute for *o*-phenylenediamine as well as the introduction of morpholine groups on benzaldehyde.

Such work suggested possible cytotoxic and antimicrobial properties of metal saphen complexes. Zn(saphen) is mildly antimicrobial (Abdel Aziz 2012), which has led to interest in developing antimicrobials based on metal saphens. Further evidence of the biological activity of these complexes was found when they were discovered to be cytotoxic. Mn(saphen) and Mn(salen) complexes selectively induce cell death in breast cancer cell lines relative to non-malignant cells (Ansari 2009). Similarly, Fe(saphen) showed selective cytotoxity to multi-drug resistant leukemia cells

(Lee 2011). In contrast, Zn(saphen) does not exhibit cytotoxic properties, suggesting the identity of the metal center is important to the biological activity of saphen complexes (Gianicchi 2013). These trials raise the possibility of using metal saphen complexes for cancer therapy, although the effects of metal saphen complexes *in vivo* have not yet been studied.

The mechanism of this cytotoxicity is likely apoptosis through the mitochondrial pathway because of cytochrome c is released from the mitochondria and the mitochondrial membrane potential is reduced (Lee 2011, Woldemariam 2008). Apoptosis may be induced by genetic damage caused by metal saphen catalyzed oxidation reactions. This would appear likely given the metal saphen complexes' ability to cleave DNA. G-quadruplex DNA in the telomeres is known to inhibit the telomerase active in tumor cells, so the stabilization of G-quadruplexes by metal saphen complexes may also play a role inducing apoptosis. Little more is known about the mechanism through which saphen complexes are biologically active. Although the kinetics of metal saphen catalysts in organic synthesis has been described, there has been no study of their biochemical kinetics.

While the biological reactivity of different derivatives with the same metal complexed has often been attempted, there have been few comparisons between the biological activities of complexes of different transition metals. Although the identity of the metal has been shown to affect cytotoxicity or plasmid cleavage, there has been no systematic attempt to compare a larger number of transition metal saphen complexes. This work seeks to systematically compare the biological activity of first row transition metal complexes except Sc(saphen) and Ti(saphen) through plasmid cleavage assays and to assess the kinetics of these reactions. The results of this assay would suggest further directions for molecular biological or *in vivo* experiments involving metal saphens.

Methods

Synthesis

The saphen ligand is produced through the condensation of salicylaldehyde and *o*-phenylenediamine to yield the imine (Fig. 2). *O*-phenylenediamine (2.5 g. 23 mM) is dissolved in 200 mL of absolute ethanol. Two equivalents (5.6 g, 46 mmol) of salicylaldehyde was added to the solution. The resulting solution was refluxed for 1.5 hours, at which point orange precipitate was observed. This precipitate was isolated by vacuum filtration and washed with water (1 x 10 mL) followed by cold diethyl ether (1 x 5 mL). This procedure yields approximately 75% yield. Additional product can be obtained through addition of distilled water to the filtrate followed by the same separation and washing procedure.

Metal-saphen complexes were formed in a methanol solution with an excess of metal (Fig. 2). Saphen ligand (100 mg) was dissolved in 20 mL of methanol and three equivalents of the corresponding metal chloride were added. The respective metal acetates and sulfates may also be used, but tend to produce somewhat lower yields. The reaction was refluxed for two hours and then the methanol solvent evaporated under reduced pressure to yield a dry paste of powder. These solid reaction products were re-suspended in distilled water (50 mL) and filtered. The solid product was then washed with 20 mL of water and allowed to dry. The product is a colored powder, with the color observed depending on the metal's identity. Complexes prepared through such methods are: V(saphen) (green, 95% yield), Cr(saphen) (dark yellow, 50% yield), Mn(saphen) (brown, 70% yield), Fe(saphen) (black-brown, 80% yield), Co(saphen) (light brown, 75% yield), Ni(saphen) (orange, 70% yield), Cu(saphen) (green, 90% yield), Zn(saphen) (yellow, 50% yield). Al(saphen) can also be produced but is water-soluble so is usually purified by chromatographic methods. All metal complexes may be stored in ambient conditions of room temperature and humidity. The procedure used for the synthesis of these saphen complexes was modified from previously published methods (Bereau 2010).

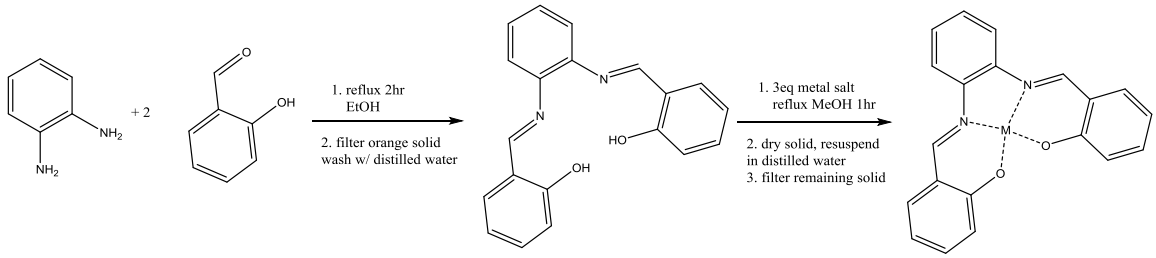

Figure 2: Synthesis of Metal Saphen Complexes

Characterization

Assuming 100% purity of product, 1 mM solutions of each complex in 100% methanol were produced and further diluted to 10 µM. These were scanned with a Varian 50 Bio UV-visible spectrophotometer at a medium scan rate (600 nm/min) from 200 nm to 800 nm (Suppl. 1)

Additionally, the solid product was analyzed with a Thermo Scientific Nicolet 15-10 reflectance FT-IR spectrometer. A total of 32 scans were performed with a 4 cm^{-1} resolution and a % transmittance spectrum was obtained for each metal complex (Suppl. 2).

For mass spectrometry, a trace amount (0.5-1.0 mg) of metal complex was dissolved in 1.5 mL HPLC grade methanol and injected into a Bruker MicroTOF ESI-MS. Time-of-flight mass spectra were obtained for each complex (Suppl. 3).

Biological Reactivity

To assess biological reactivity, a plasmid cleavage assay was used. Both 10 µM and 1 µM aqueous solutions of each metal saphen complex, as well as uncomplexed saphen were prepared. In the first step, 10 µL reactions were prepared with the following concentrations: 5 µM plasmid, 200 nM saphen complex, and the presence of one of the following: 1 mM ascorbate, 1 mM hydrogen peroxide, 1 mM ascorbate and peroxide, or neither. An aqueous solution of 20 mM HEPES buffered at pH=7.4 was used as the solvent. All reactions were run under ambient conditions at atmospheric pressure. The reactions were allowed to proceed for 1 hr at room temperature and the resulting reaction mixtures separated by 1% agarose gel electrophoresis.

In addition, for each saphen complex similar 10 µL reactions was prepared with 500 nM complex and time as the dependent variable to determine final rates. Time points were collected at 5, 10, 15, 30, 45, 60, 90, and 120 minutes. The concentration of each saphen complex was also varied while maintaining a complex concentration of 5 µM and reaction time of 1 hour. Concentrations used were 200 nM, 300 nM, 400 nM, 500 nM, 1 µM, and 2 µM of each of the saphen complexes. As before, the reactions were carried out in the presence of 1 mM ascorbate, 1 mM hydrogen peroxide, both, or neither. Reactions were characterized by 1% agarose gel containing GelRed.

Whenever agarose gel electrophoresis was used, 5 µL of reaction mixture was loaded in each well. A 1% agarose gel with GelRed stain was run at 90 V for 30-45 minutes to achieve good separation.

The intensity of each band observed under UV light was quantified using ImageJ software and a correction factor of 1.47 was applied to the intensity of supercoiled bands to account for the limited ability of GelRed or Ethidium Bromide to bind to supercoiled DNA (*8*). The fraction of the total intensity observed in a band and the known total concentration of plasmid was used to calculate the concentration of each respective band. From this concentration data, kinetics curves were fitted.

Results/Discussion

UV-Visible Spectroscopy

The spectrum of V(saphen) suggests multiple charge-transfer transitions around 300 nm and 410 nm. As an illustrative case, the actual spectrum as well as that of the free ligand is also included (Fig. 3). The spectra for other metal saphen complexes are found in the supplementary material (Supp. 1). The spectrum agrees with previous results reporting an intense, broad charge transfer

transition centered at 419 nm. (Mohebbi & Bakhshi 2008). The experimental molar absorptivity of 7000 M^{-1} cm^{-1} is different from the reported value of 10700 (Mohebbi & Bakhshi 2008), but the solvent used in the reported value is DMF rather than methanol. The d-d transition at 545 nm was not observed, but this is reported to be a weak absorbance maximum.

On inspection, the Cr(saphen) spectrum is highly similar to that of the ligand, suggesting the free ligand may be present in the sample. Additionally, the absorbance maximum reported at 376 nm does not appear to be present, or perhaps it is shifted to 340 nm (Venkataramanan 2003). Literature does not report molar absorptivities for Cr(saphen) complex in relevant solvents.

Mn(saphen)'s spectrum is characterized by maxima at 240, 340, and 425 nm. While detailed discussion of the UV-Visible spectrum of non-derivatized Mn(saphen) could not be identified through a literature search in SciFinder, its spectrum can be interpreted as a π-π^* transition at 240nm and a charge transfer transitions at 340 nm. The two transitions have similar intensity and the 340 nm one is particularly broad, suggesting the 340 nm peak represents a charge transfer.

Fe(saphen)'s spectrum is somewhat similar to that of Mn(saphen), with peaks at 295 nm, 360 nm, and a very weak maximum around 600 nm, the latter corresponding to the Fe d-d transition. Reported spectra suggest a doublet instead of the single peak at 295 nm; this may be a solvent effect or relevant to the purity of the sample (Liu 2007). The observed molar absorptivity of the 295nm peak is very high—approximately 30,000 M^{-1} cm^{-1}, which is actually higher than the reported values for the two peaks reported (17,000 and 15,000 M^{-1} cm^{-1}) (Liu 2007)

Co(saphen)'s spectrum is unique in that it features a single peak around 320 nm and a gradual decline in absorbance with increasing wavelength featuring multiple shoulders. The shoulders observed correspond with the reported absorbance maxima at 315 and 385 nm, but the molar absorptivities of less than 5000 M^{-1} cm^{-1} observed are significantly smaller than the values reported, which are always above 10000 M^{-1} cm^{-1} (Mehta 2004). This may reflect the choice of solvent; reported values are for THF solution while the spectra were acquired in methanol solution. In addition, the small shoulder observed at 465 nm has also been reported (Pradhan 2010) and is likely due to a d-d transition.

Ni(saphen) has three prominent absorbance maxima at 250 nm, 300 nm, 370 nm, and 470 nm. These correspond to reported peaks (Mehta 2004, Pradhan 2010). As is the case with Co(saphen), the molar absorptivities reported in THF do not correlate with those observed in methanol.

Cu(saphen) and Zn(saphen) feature prominent charge-transfer transitions. Cu(saphen)'s transitions at 310 nm and 425 nm and Zn's transitions at 300 nm and 400 nm correspond to reported values (Pradhan 2010). Molar absorptivities for these spectra could not be found.

Due to the lack of sufficient reported values for molar absorptivities, further characterization methods were pursued. The UV-Visible Spectra for each compound may be found in the supplemental material (Suppl. 1). In general, the UV-Visible spectra supported the identity of each product. The only exception was Cr(saphen), in which case the product may contain unreacted ligand.

FT-IR Spectra

The observed IR peaks were compared to reported values for IR bands to further assess purity (Table 1). Additionally, the raw IR spectra are included as a supplement (Supp. 2) The IR spectra matched very well with reported spectra for the Mn, Fe, Co, Ni, and Cu, complexes (Pradhan 2010). For Zn(saphen), the observed spectrum matched well with the reported spectrum, although there were some slight shifts (Pradhan 2010). V(saphen) was identified by the presence of a characteristic V=O stretch at 982 cm^{-1} as well as the shift on the C=N stretching vibration (Mohebbi & Bakhshi 2008). No detailed discussion of Cr(saphen)'s IR spectrum could be found through a literature search.

An excellent match between reported and observed peaks without the presence of extraneous peaks suggests the sample is pure and corresponds to the metal complex. For all complexes except

Zn, IR spectroscopy further supported the purity of the material. The observed and reported values of the IR bands are identified in Table 1.

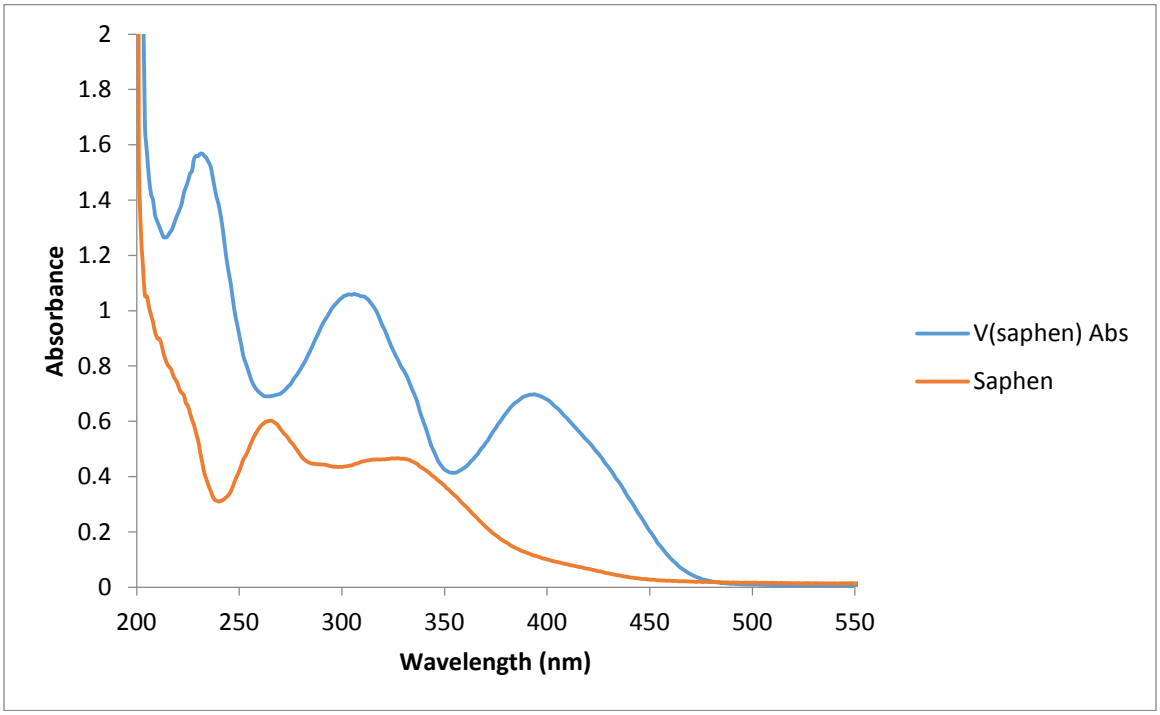

Figure 3: V(saphen) UV-Visible Spectrum

Table 1: IR Spectra of Saphen Complexes	
Metal	IR peaks in cm-1: experimental (assignment from Pradhan 2010)
V	1603 (C=N stretch 1603), 975 (V=O stretch 982)
Mn	1577 (1560), 1528 (1534), 1489 (1481), 1461 (1461), 1433 (1432), 1375 (1375), 1315 (1316), 1275 (1276), 1191 (1192), 1145 (1150), 1102 (1096), 1028 (1029), 924 (910), 874 (883), 858 (854), 810 (810), 759 (752), 746 (741), 668 (668)
Fe	1603 (C=N stretch 1604),1578 (1578), 1533 (1536),1461 (1461),1378 (1379), 1313 (1314), 1194 (1196), 1145 (1150), 810 (812), 747 (759), 611(614)
Co	1611 (C=N stretch 1613), 1579 (1581), 1525 (1528), 1459 (1461), 1433 (1440), 1375 (1378), 1331 (1329), 1203 (1191), 1155 (1150), 1127 (1130), 1037 (1030), 806 (810), 750 (720), 670 (668)
Ni	1604 (C=N stretch 1608),1577 (1578), 1515 (1521), 1491 (1491),1457 (1458),1441 (1443), 1372 (1372), 1336 (1341), 1262 (1265), 1235 (1235), 1194 (1195), 1148 (1150), 1127 (1127), 1021 (1021), 926 (930), 844 (849), 754 (756), 619 (619)
Cu	1607 (C=N stretch 1600), 1576 (1576), 1548 (1559), 1526 (1533), 1488 (1483), 1458 (1461), 1444 (1444), 1378 (1374), 1308 (1316), 1258 (1260), 1248 (1245), 1146 (1142), 1039 (1040), 863 (858), 803 (807), 749 (756), 661 (668)
Zn	1604 (C=N stretch 1614), 1579 (1585), 1530 (1540), 1468 (1462), 1444 (1445), 1375 (1386), 1310 (1324), 1242 (1244), 1202 (1180), 1152 (1152), 1127 (1126), 1024 (1031), 844 (853), 807 (820), 742 (748)

Note: Spectra for each compound are reported in supplement 2.

Table 2: Mass Spectra of Saphen Complexes		
Complex	Major m/z observed	Identification
V(saphen)	404.0 785.0	V=O(saphen)Na and V=O(saphen)$_2$Na
Cr(saphen)	366.0 317.1	Cr(saphen) saphen
Mn(saphen)	369.0	Mn(saphen)
Fe(saphen)	370.0	Fe(saphen)
Co(saphen)	373.0 317.1	Co(saphen) saphen
Ni(saphen)	395.0 767.0	Ni(saphen)Na Ni(saphen)$_2$Na
Cu(saphen)	381.3 400.0 779.0	Cu(saphen) Cu(saphen)Na Cu(saphen)$_2$Na
Zn(saphen)	379.0 317.1	Zn(saphen) Saphen

Note; The mass spectra are reported in Supplement 3.

Mass Spectrometry

In all cases, the major peaks observed in the mass spectra of saphen complexes corresponded to the molecular ions of the expected products of the reaction (Table 2). Actual spectra are included as a supplement (Supp. 3). A peak corresponding to uncomplexed saphen ligand was found in the Cr, Co, and Zn complexes. In terms of relative intensity, the saphen peak was strongest in the case of Cr(saphen) and Zn(saphen), while it was a minor peak in Co(saphen). This suggests the Cr and Zn products may be impure.

Frequently, the complexes flew as sodium adducts or dimmers in solution. This phenomenon is common in ESI-MS and does not necessarily imply the formation of dimers. In the case of the V complex, the oxide identified on IR was also observed on MS. The preceding table summarizes the assignment of mass spectrometry peaks (Table 2).

General Comments on Purity

Data from UV-Visible spectroscopy, IR, and MS converge to support the purity of the V, Mn, Fe, Ni, and Cu complexes prepared. These complexes appear to be of high purity. In the case of Co(saphen), mass spectrometry indicates the presence of some uncomplexed saphen, while the other methods support its purity. Due to the much poorer match of the Zn(complex) IR spectrum with published data and the presence of uncomplexed saphen on MS, there appears to be contamination with ligand. While there is no suitable IR reference data, the similarity between the UV-Visible spectrum of Cr(saphen) and the strength of the uncomplexed saphen molecular ion peak on MS, it appears this product also contains non-complexed ligand.

Although non-complexed ligand was identified in the case of Cr(saphen) and Zn(saphen), these products were still used in biological experiments. Since a non-complexed ligand control was used in the biological experiments, it is still possible to differentiate between any effects attributed to the saphen itself. In addition, the percent total intensity was used in analysis of plasmid cleavage. Concentration ratios ought not to be affected by impurity, provided that all parts of the complex prepared are equally impure.

Biological Reactivity: Cleavage of pUC19 Plasmid

General Observations of Gels

pUC19 plasmid is normally supercoiled—that is the state it is found in the bacterial cytoplasm as well as in solution. When pure plasmid is run on an agarose gel, three bands are generally observed. The farthest running and strongest corresponds to supercoiled plasmid. The next band, the weakest, consists of linearized plasmid, while the shortest-running band is nicked plasmid. When some agent cleaves the DNA strand of pUC19, one observes the strengthening of the nicked and linear bands and a weakening of the supercoiled band. Indeed, this was observed under oxidative and oxidative-reducing conditions. A visualized gel showing the degradation of pUC19 by Ni(saphen) is included to illustrate this process (Fig. 4-5). Additional Gels are included in the supplement (Supp. 4).

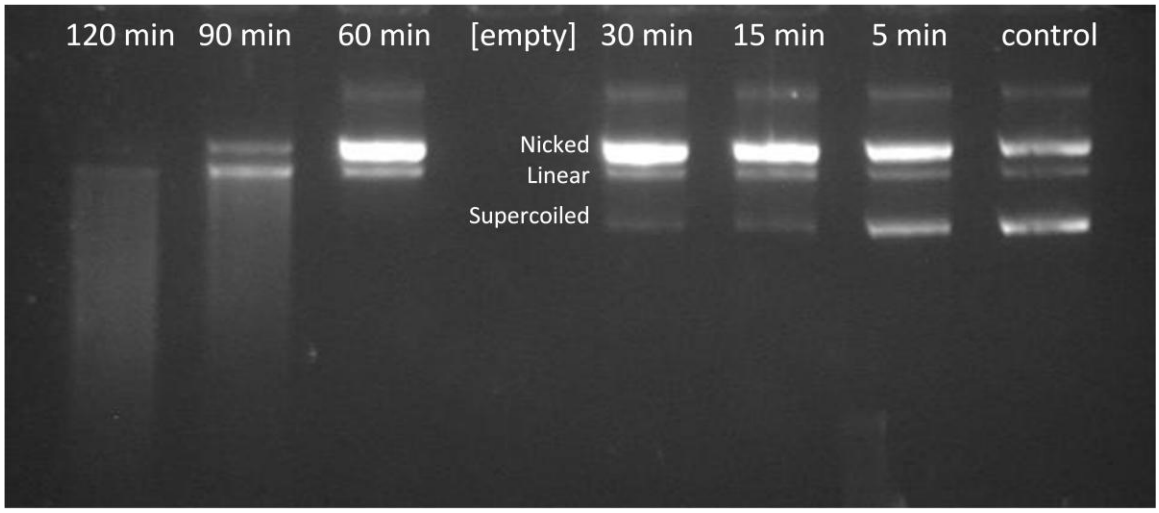

Figure 4. Time Dependence Gel for Ni(saphen) under Oxidative-Reducing Conditions. Reaction Conditions: 1 mM H_2O_2, 1 mM ascorbate, 5 µM pUC19, 500 nM Ni(saphen), 20 mM HEPES, 200 mM NaCl, pH=7.4. Gel Conditions: 1% agarose in TAE stained with GelRed, 90V applied for 60 min.

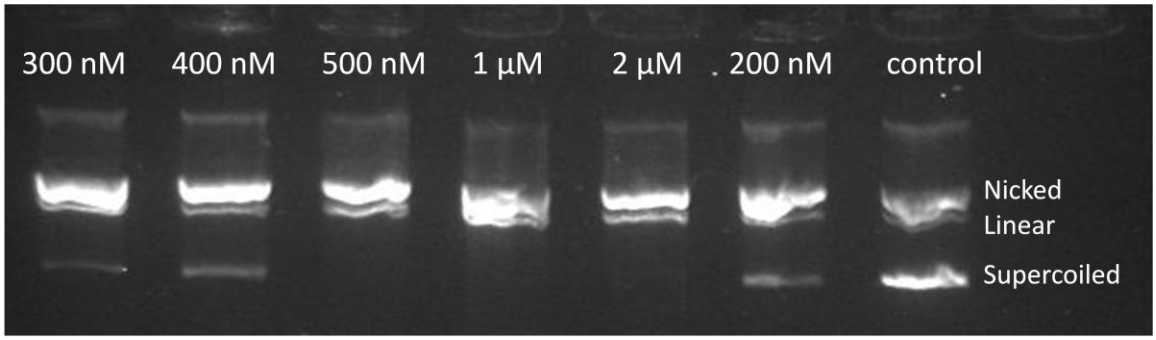

Figure 5. Concentration Dependence Gel for Ni(saphen) under Oxidative-Reducing Conditions Reaction Conditions 1 µM ascorbate, 1 µM H_2O_2, 5 µM pUC19, 20 mM HEPES, 100 mM NaCl, pH=7.4, reaction time= 60 min. Gel Conditions: 1% agarose in TAE stained with GelRed, 90V applied for 45min

Reducing Conditions

When pUC19 was incubated with saphen complexes in 1 mM buffered ascorbate, no statistically significant difference between the complexes, saphen ligand, and control conditions for either time-dependent or concentration-dependent gels. Indeed, there was little plasmid leavage observed at all. This suggests that a reducing co-reagent will not lead to plasmid cleavage.

Oxidative Conditions

Under 1 mM buffered peroxide conditions, a significant difference was observed between the rate of cleavage for control conditions of either plasmid in buffer or saphen ligand and plasmid in buffer and each saphen complexes. While each of the complexes cleaved supercoiled saphen at a faster rate than controls, it was not possible to differentiate between the rates of decay for different complexes, i.e. each complex appeared to decay pUC19 at a equal rate that was higher than that of control. This may be observed in the decay curve Fig. 6. This inability to see a difference between complexes is probably due to the slow reaction rate. At the same time, there was no significant difference observed in the concentration-dependence experiment between metal saphens and controls and no overall concentration dependence was observed.

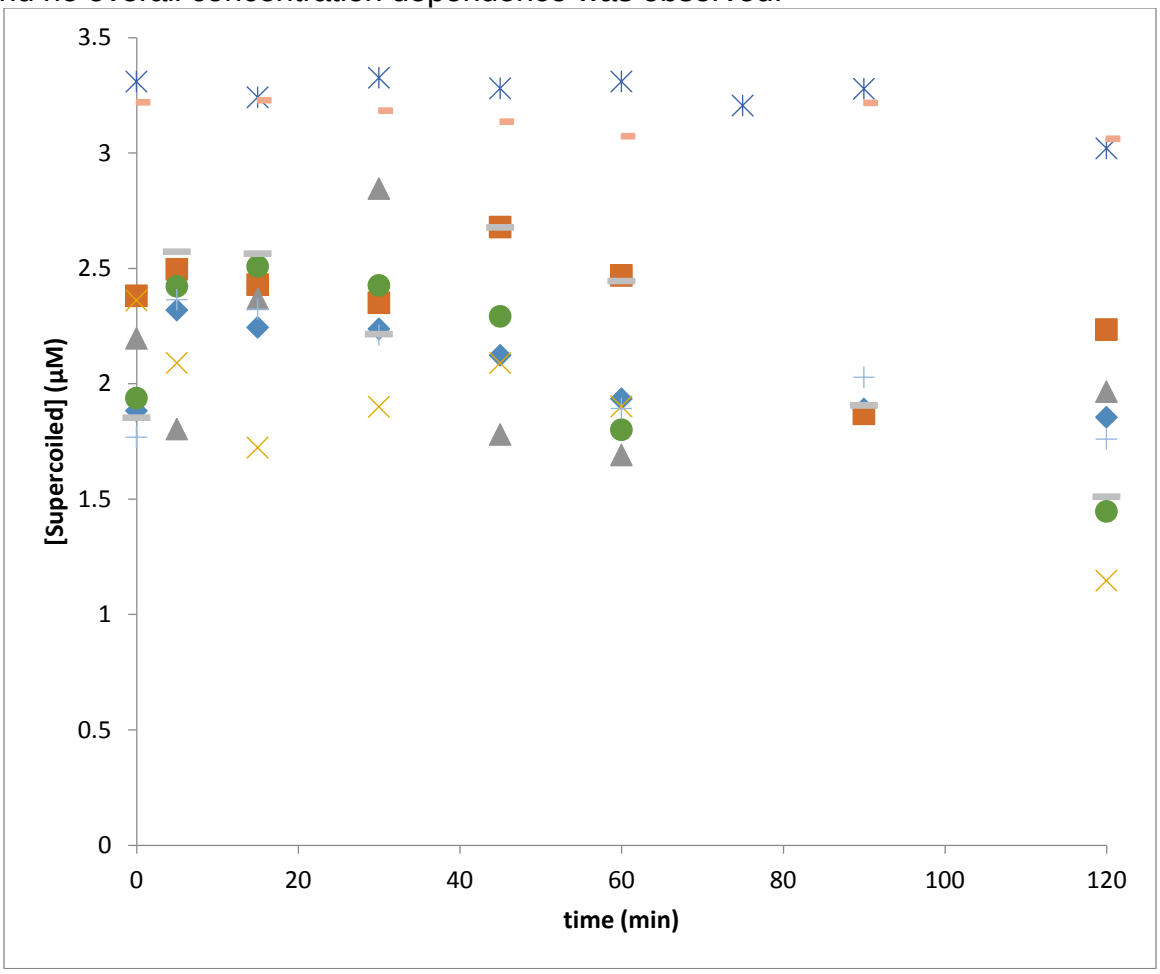

Figure 6. Decay of Supercoiled Plasmid under Oxidative Conditions

Reaction Conditions: 500 nM metal(saphen) 1 µM H_2O_2, 20 mM HEPES, 100 mM NaCl, pH=7.4
Key: blue diamond=Co(saphen), orange square=Cr(saphen), gray triangle=Cu(saphen), orange "X"=Fe(saphen), blue asterisk=control, blue cross=Ni(saphen), orange bar=saphen ligand, gray bar=V(saphen)

Oxidative-Reductive Conditions

Under conditions of both oxidative and reducing agent, 1 mM hydrogen peroxide and 1 mM ascorbate buffer, the reaction rate was significantly increased. This allowed for quantitative analysis to obtain kinetic data. The data from the concentration-dependence experiments was used to find the average rate of decay of supercoiled plasmid for the first hour of reaction. This was assumed to be similar to the initial rate of reaction and plotted against the concentration of metal saphen complex to form a first-order plot. A fit to equation 1 was obtained for the decay of the supercoiled plasmid in the presence Cu, Fe, Mn, Ni, and V complexes (Fig. 7) and the rate constants were calculated (Table 3).

Parabolic fits to the second-order rate raw matched the concentration dependence data significantly poorer and were not further pursued.

$$\text{Equation 1: rate} = -\frac{d[S_c]}{dt} = k_{sc}[\text{complex}]$$

Table 3: First-Order Rate Constants for Cleavage of Supercoiled pUC19		
Metal	k_{sc} (min^{-1})	R^2
Cu	0.07±0.06	0.554
Fe	0.22±0.02	0.992
Mn	0.076±0.007	0.970
Ni	0.085±0.005	0.984
V	0.06±0.02	0.668

Data obtained from oxidative-reducing raction conditions and fitting to equation 1.

While a statistically significant difference was obtained between Fe(saphen) and the other complexes, a paired t-test between the first-order rate law data for Cu(saphen) or V(saphen) and Ni(saphen) only yielded p=0.07. This suggests that Fe(saphen) and possibly Cu(saphen) or V(saphen) leads to plasmid cleavage at a significantly higher rate than the other complexes.

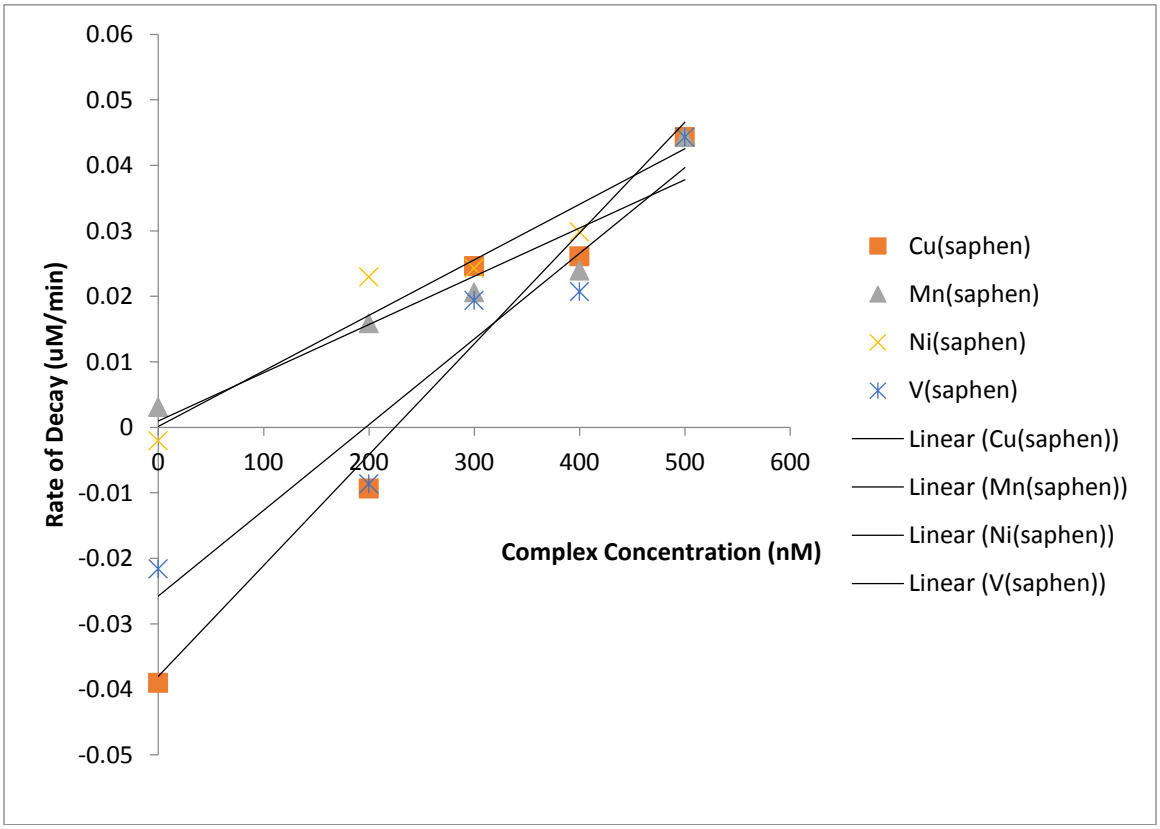

Figure 7. First Order Rate Law for the decay of Supercoiled Plasmid
Note: Data for Fe(saphen) not included for comparison.

The concentration versus time data was fitted to the following two-step degradation process: $S_c \rightarrow N_k \rightarrow L_n$ with a unimolecular rate constant of k_1 for the first step and another unimolecular rate constant k_2 for the second step. This results in the following rate laws (Eqn. 2-3). The initial growth in the concentration of linear plasmid was also fitted to an exponential growth model (Eqn. 4).

$$\text{Equation 2.} [S] = [S]_0 e^{-k_1 t}$$

$$\text{Equation 3. } [N] = [S]_0 \left(\frac{k_1}{k_2 - k_1}\right)\left(e^{-k_1 t} - e^{-k_2 t}\right) + [N]_0\left(1 - e^{-k_2 t}\right)$$

$$\text{Equation 4. } [L] = [L]_0 e^{-k_{2obs} t}$$

Where [L]=concentration linear plasmid, [N]=concentration nicked plasmid, and [S]=concentration supercoiled plasmid. Note the last rate law only models the initial exponential growth of linear plasmid.

Regression analysis was done using Origin 7 software. While good fits were found for the exponential decay of the supercoiled plasmid, significantly worse fits were obtained for the nicked and linear concentrations using equations 3-4. An example is given for the Cu(saphen) complex (Fig. 8a-c). The results of regression analysis are given in the following table (Table 4)

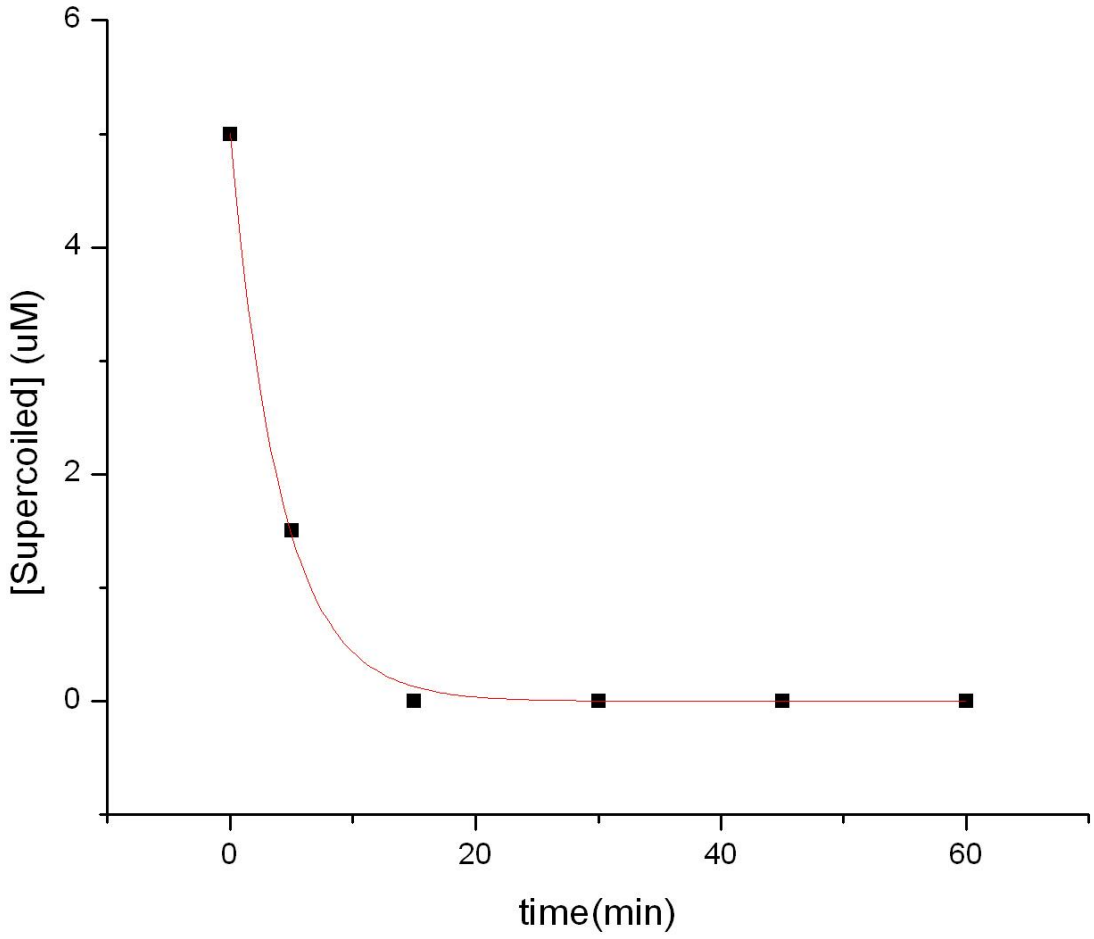

Figure 8. Fitting supercoiled plasmid time dependence data to equation 2 for 500 nM Cu(saphen) conditions.

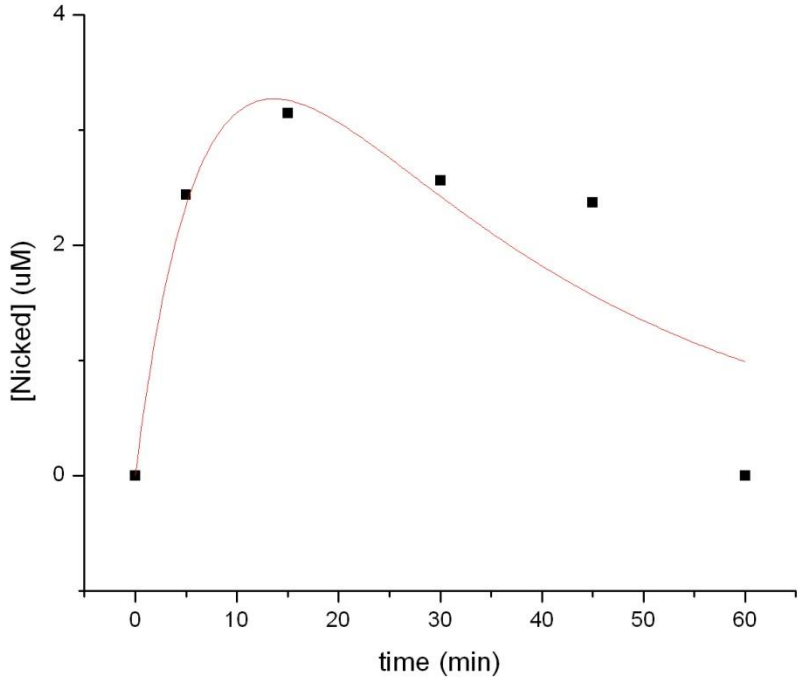

Figure 8. Fitting of nicked plasmid time dependence data to equation 3 for 500 nM Cu(saphen) conditions.

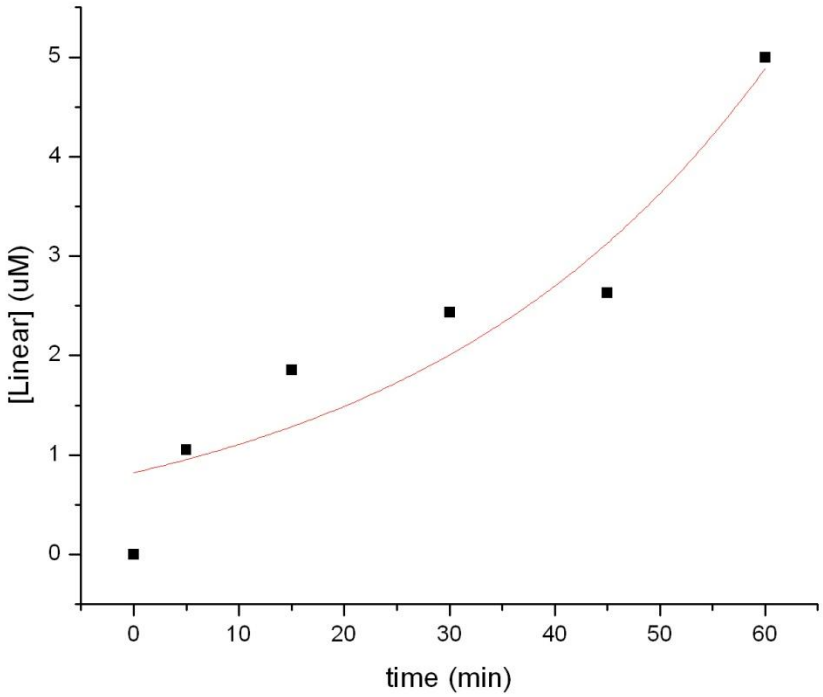

Figure 9. Fitting of supercoiled plasmid time dependence data to equation 4 for 500 nM Cu(saphen) conditions.

Table 4: Rate Constants for Cleavage of pU19				
Compound	Supercoiled	Nicked		Linear
	k_1 (min^{-1})	k_1 (min^{-1})	k_2 (min^{-1})	k_{2obs} (min^{-1})
Co(saphen)	0.031(6)	*no fit*		0.0103(4)
Cu(saphen)	0.245(9)	0.14(5)	0.031(6)	0.026(4)
Fe(saphen)	0.068(12)	*no fit*		0.01864(17)
Mn(saphen)	0.03(1)	0.13(8)	0.005(6)	0.018(4)
Ni(saphen)	0.036(7)	0.02(6)	0.2(4)	0.0147(9)
V(saphen)	0.043(8)	0.026(4)	0.023(4)	0.039(2)
saphen	0.061(5)	0.08(3)	0.009(4)	0.0406(18)
control	0.0115(6)	*no fit*		0.025(2)

Data obtained from oxidative-reducing reaction conditions and fitting to Equations 2-4

The rate constants calculated suffer from low precision, but in the case of V(saphen), Cu(saphen) and Mn(saphen) there are significant differences between the k_1 obtained from the time dependence data for supercoiled and nicked plasmid. This suggests the model chosen may not adequately explain the further cleavage of pUC19, or the data was compromised by excessive fragmentation of the plasmid. When the plasmid is allowed to degrade too far, many small fragments are formed which do not appear on the gel visualization. This is expected to introduce error in the results by artificially inflating the calculated concentration.

If only the higher-precision results for the exponential decay/growth of supercoiled plasmid are taken, the metal saphen complexes seem to segregate into three approximate groups in terms of k_1. The first, Co, Mn, Ni, and V, have k_1's around 0.03 min^{-1} which do not differ in a statistically significant way. The next, Fe(saphen) and saphen ligand, have higher k_1's around 0.06 min^{-1} and finally, Cu(saphen), an outlier at k_1=0.245 (min^{-1}). This does not quite agree with the k_1 obtained from the nicked dataset, although even this value of 0.14 min^{-1} is significantly greater than others.

The pattern that emerges is that the ligand control has a rate constant determined to be greater than or equal to that of most of the metal complexes. This is interesting, since under peroxide conditions the ligand control had a time dependence curve equivalent to that of plasmid control but different from that of the metal complexes. One possibility is that the saphen ligand is coordinated to trace amounts of metal in the solution and reacts with the plasmid. The reactions observed were quite fast; after 1hr there was already evidence of fragmentation. Again, the presence of small fragments may lead to error in the calculated concentrations of plasmid.

The rate constants for the second degradation step k_{2obs} were generally smaller than the k_1 constants, suggesting that cleavage of supercoiled DNA is faster than the cleavage of nicked DNA. P=0.07 for a one-tailed paired t-test comparing k_1 and k_2 values, suggesting this difference may or may not be significant. The two rate constants are not correlated; although Cu(saphen) has the highest k_1 rate it has a relatively small k_{2obs}.

Discussion and Future Directions

Modifying the conditions from reducing, oxidative, and oxidative-reducing had the largest effect on the cleavage of plasmid. Under reducing conditions of 1 mM ascorbate, no degradation of the plasmid was observed in two hours, while under oxidative conditions of 1 mM hydrogen peroxide the metal(saphen) complexes cleaved plasmid at a significantly higher rate than controls. The addition of both hydrogen peroxide and ascorbate yielded dramatic increases in reaction rates. At the same time, rates for metal(saphen) complexes were no longer different from those of saphen ligand control, but the first-order rate constant for the decay of supercoiled plasmid was significantly greater for metal(saphen) or saphen than control.

Greater success was achieved by fitting the decay of supercoiled plasmid to first-order curves with respect to both the metal (saphen) complex and supercoiled plasmid. Analysis of the time dependence data for nicked and linear plasmid yielded equivocal results, however. In terms of comparison between the different complexes, it appears that Cu(saphen) has a particularly large rate constant derived from time dependence data while Fe(saphen) has a particularly large rate constant with derived from concentration dependence data. Fe(saphen) and Cu(saphen) also appear to have relatively large rate constants with respect to nicked plasmid compared to other complexes.

The first-order kinetics with respect to metal complex and supercoiled plasmid suggest a bimolecular process by which the supercoiled plasmid and complex must enter close physical proximity. Since cleavage only occurs under oxidative conditions, and its rate is significantly increased by a reducing co-reagent, one may infer that the reaction occurs through a process by which the metal is both oxidized and cleaves the DNA. When the reducing co-reagent is present, a kind of catalytic cycle could occur in which the metal is reduced to react again with another DNA. In this case, further study may reveal the metal complex displays enzyme-like kinetics.

The study of a catalytic cycle outside an enzyme is important, and there are many well known examples such as Fe^{2+} and peroxide, known as Fenton's reagent (Chen 2011). Such a catalytic cycle would explain the relatively small concentrations at which metal-saphen complexes are cytotoxic. It also explains why plasmid cleavage under oxidative-reducing conditions could be observed at concentrations of as low as 200-500 nM rather than 1-1000 μM as was previously reported (Woldemariam 2008). More importantly, further study of the kinetics of this reaction would give insights towards this compound's apparent cytotoxicity. In particular, a more accurate method of quantifying the percentage of linear and supercoiled DNA is needed. This could be achieved through following of the melting temperature or possibly by observing shifts in the UV-Visible absorbance spectra. These follow-up experiments would be valuable and represent the future plans of this researcher. They are of particular importance since they could replicate or refute the observation that only metal(saphen) complexes cleave DNA better than controls in oxidative conditions but naked ligand may also cleave DNA better than control under oxidative-reducing conditions.

The differing reaction rates observed between complexes is likely related to the differing reduction potentials. Another follow-up experiment using cyclic or hydrodynamic voltammetry to assess the reduction potentials may be necessary, and the complexes, although not water-soluble, readily dissolve in other polar solvents suitable for voltammetry.

Additionally, further interest may be directed towards the degradation of DNA by the Cu(saphen) and Fe(saphen) complexes in particular. Rather than use agarose gel electrophoresis to separate the reaction products, mass spectrometry may be used to analyze plasmid fragmentation. This could yield insights into the further fragmentation of plasmid beyond linearization, which is impossible to visualize on electrophoresis due to the random nature of the fragment lengths producing a continuum (or streak on the gel). The cytotoxic properties of Cu(saphen) complexes may also be investigated, since Cu(saphen) appears to be particularly effective at cleaving DNA but its effect on mammalian cells has yet to be investigated.

It is worthwhile to note that many different ligands can be readily prepared within the saphen class using commercially available derivatives of *o*-phenylenediamine and salicylaldehyde. A more systematic exploration of the metal complexes of the saphen class may be valuable. In particular, the ligand can be varied to further increase the rate of cleavage for Cu(saphen) and Fe(saphen).

References

1. Abdel Aziz, A; Badr, I; El-Sayed, I. Synthesis, Spectroscopic, [and] Photoluminescence Properties and Biological Evaluation of Novel Zn(II) and Al(III) Complexes of NOON Tetradentate Schiff Bases. *Spectrochim. Acta A*, **2012**, *97*, 388-396.

2. Ansari, K; Kasiri, S; Grant, J; Mandal, S. Apoptosis and Anti-Tumor Activities of Manganese(III)-salen and –salphen Complexes. *Dalton Trans.* **2009**, 8525-8531.
3. Bahaffi, S; Abdel Aziz, A; El-Naggar, M. Synthesis, Characterization, DNA Binding Ability and Antibacterial Screening of Copper(II) Complexes of Symmetrical NOON Tetradentate Schiff Bases Bearing Different Bridges. *J. Molec. Struct.* **2012**. *102*, 188-196.
4. Bereau, V; Jubera, V; Arnaud, P; Kaiba, A; Guionneau, P; Sutter, J. Modulation of the Luminescence Quantum Efficiency for Blue Luminophor {Al(salophen)}+ by ester substituents. *Dalton Trans.* **2010*,*** *39*, 2070-2077
5. Campbell, N; Karim, N; Parkinson, G; Gunaratnam, M; Petrucci, V; Todd, A; Vilar, R; Neidle, S. Molecular Basis of the Structure-Activity Relationships between Salphen Metal Complexes and Human Telomeric DNA Quadruplexes. *J. Med. Chem.* **2012**, *55* (1), 209-222
6. Chen, L; Ma, J; Li, X; Zhang, J; Fang, J; Yinghong, G; Xie, P; Strong Enhancement on Fenton Oxidation by Addition of Hydroxylamine to Accelerate the Ferric and Ferrous Iron Cycles. *Environ. Sci. Technol.* **2011**, *45* (9), 3925-3930.
7. Coletti, A; Galloni, P; Sartorel, A; Conte, V; Floris, B. Salophen and Salen Oxo Vanadium Complexes as Catalysts of Sulfides' Epoxidation with H_2O_2: Mechanistic Insights. *Catalysis Today*. **2012**. *192*, 44-55.
8. Gianicchi, I; Brissos, R; Ramos, D; Lapuente, J; Lima, J; dalla Cort, A; Rodriguez, L. Subsituent Effects on the Biological Properties of Zn-Salophen Complexes. *Inorg. Chem.* **2013**, *52*, 9245-9253.
9. Joyner, J; Keuper, K; Cowan, J. DNA Nuclease Activity of Rev-coupled Transition Metal Chelates. *Dalton Trans.* **2012**, *41*, 6567-6578.
10. Lee, S; Hille, A; Kitanovic, I; Jesse, P; Henze, G; Wolfl, S; Gust, R; Prokop, A. [Fe^{III}(salophene)Cl], A Potent Iron Salophene Complex Overcomes Multiple Drug Resistance in Lymphoma and Leukemia Cells. *Leukemia Res.* **2011**, *35*, 387-393.
11. Li, M; Lan, T; Lin, Z; Yi, C; Chen, G. Synthesis, Characterization, and DNA Binding of a Novel Ligand and its Cu(II) Complex. *J. Biol. Inorg. Chem.* **2013**, *18*, 993-1003.
12. Liu, J; Zhang, B; Wu, B; Zhang, K; Hu, S. The Direct Electrochemical Synthesis of Ti(II), Fe(II), Cd(II), Sn(II), and Pb(II) Complexes with N, N'-Bis(salicylidine)-o-phenylenediamine. *Turk. J. Chem.* **2007**, *31*, 623-629.
13. Mehta, B; Joishar, D. Synthesis and Spectral Properties of Cobalt(II) and Nickel(II) Complexes Derived from Bidentate Schiff Bases. *Asian J. Chem.* **2004**, *16*, 910-916.
14. Mohebbi, S; Bakhshi, B. Electrochemical and Spectral Behavior of Mononuclear Oxo-Vanadium(IV)salicyldiimine Complexes. *J Coord. Chem.* **2008***, 61* (*16*), 2615-2628.
15. Pradhan, K; Selvaraj, K; Nanda, A. A Convenient Approach to the Synthesis of Different Types of Schiff's Bases and Their Metal Complexes. *Chem. Lett.* **2010**, *39*, 1078-1079 [Suppl. Materials.]
16. Shitama, H; Katsuki, T. Asymmetric Epoxidation Using Aqueous Hydrogen Peroxide as Oxidant: Bio-Inspired Construction of Pentacoordinated Mn-salen Complexes and their Catalysis. *Tetrahedron Lett.* **2006,** *47*, 3203-3207.
17. Venkataramanan, N; Premsingh, S; Rajagopal, S; Pitchumani, K. Electronic and Steric Effects on the Oxidation of Sulfides and Sulfoxides with Oxo(salen)chromium(V) Complexes. *J. Org. Chem.* **2003**, *68*, 7460-7470.
18. Woldemariam, G; Mandal, S. Iron(III) Salen Damages DNA and Induces Apoptosis in Human Cells via Mitochondrial Pathway. *J. Inorg. Biochem.* **2008**, *102*, 740-747.
19. Wu, G; Wang, X; Liu, X; Ding, K; Zhang, F; Zhang, X; Environmentally Benign Oxidation of Benzyl Alcohol Catalyzed by Sulphonato-Salphen-Chromium(III) Complexes Immobilized on MCM-41. *Catal. Lett.* **2014**, *144*, 364-371.